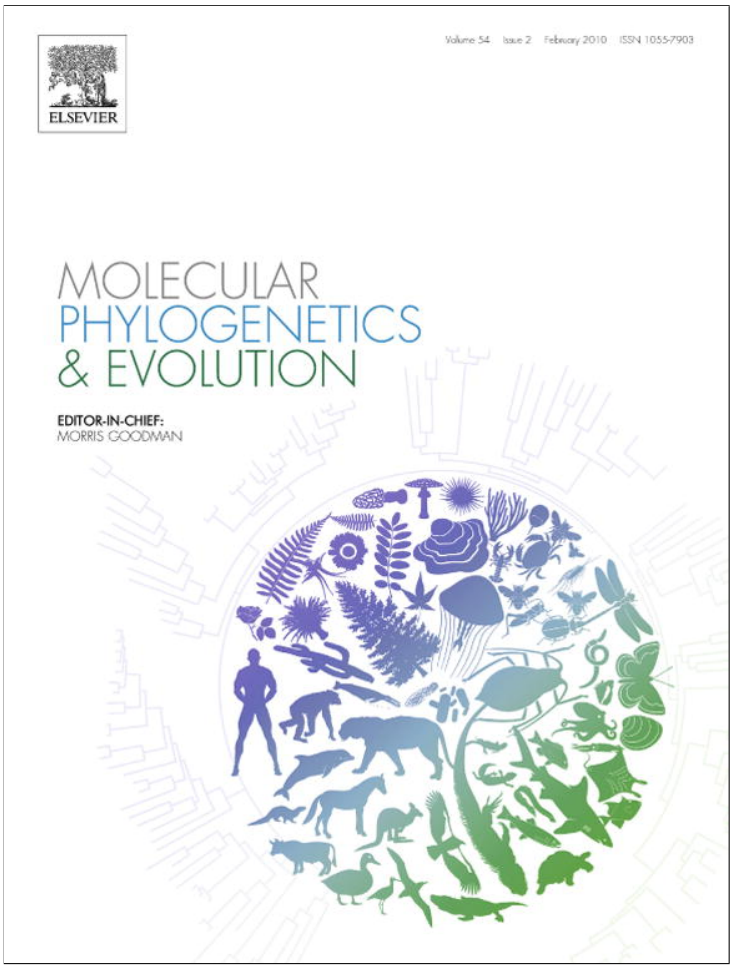

Molecular Phylogenetics and Evolution 54 (2010) 594–606

Contents lists available at ScienceDirect

Molecular Phylogenetics and Evolution

journal homepage: www.elsevier.com/locate/ympev

Quaternary range dynamics and polyploid evolution in an arid brushland plant species (*Melampodium cinereum*, Asteraceae)

Carolin A. Rebernig [a], Hanna Weiss-Schneeweiss [a], Gerald M. Schneeweiss [b,*], Peter Schönswetter [b], Renate Obermayer [a], José Luis Villaseñor [c], Tod F. Stuessy [a]

[a] Department of Systematic and Evolutionary Botany, University of Vienna, Rennweg 14, A-1030 Vienna, Austria
[b] Department of Biogeography and Botanical Garden, University of Vienna, Rennweg 14, A-1030 Vienna, Austria
[c] Instituto de Biología, Departamento de Botánica, Universidad Nacional Autónoma de México, Tercer Circuito s/n, Ciudad Universitaria, Delegación Coyoacán, MX-04510 México DF, México

ARTICLE INFO

Article history:
Received 26 May 2009
Revised 2 October 2009
Accepted 6 October 2009
Available online 13 October 2009

Keywords:
Aridification
Bayesian hypothesis testing
Phylogeography
Polyploidy

ABSTRACT

Pleistocene climatic fluctuations played a principal role for range formation and population history of many biota, including regions not directly affected by glaciations, such as the arid habitats of the southwestern United States and adjacent Mexico. Specifically, drought-adapted species are expected to have persisted during cooler and wetter periods in one or more refugia, resulting in lineage differentiation, from where they reached their current distribution after range expansion in the course of Holocene aridification. Here, we test this hypothesis using *Melampodium cinereum* (Asteraceae), a morphologically and cytologically variable species of dry brushlands of Texas and adjacent Mexico. In line with the hypothesized presence of several refugia, AFLP data provide strong evidence for the presence of geographically distinct genetic lineages, which, however, only partly agree with current intraspecific taxonomy. Despite multiple origins, tetraploids form a genetically cohesive group. The exclusive occurrence of tetraploids in a range parapatric to that of the diploids likely results from former geographic isolation of cytotypes, lending further support for the presence of Pleistocene refugia. Whereas plastid sequence data show a clear signal for the expected Holocene range and population expansion, they show little geographic structure and high levels of intrapopulational diversity. This may be due to lineage sorting during periods of population separation and/or substantial gene flow among populations via seeds, which has not been sufficient to erode the overall pattern of genetic divergence resulting from geographic isolation.

1. Introduction

Phylogeography infers past population processes in a geographical context and determines the processes underlying the origin, distribution and maintenance of biodiversity (Beheregaray, 2008). Its success over the past two decades has been spurred by conceptual, methodological and computational advances allowing testing of explicit models (statistical phylogeography: Knowles and Maddison, 2002; Knowles, 2004) with increasingly sophisticated tools (e.g., Bayesian skyline plot and Bayesian skyride: Drummond et al., 2005; Minin et al., 2008).

Numerous phylogeographic studies have shown the important role of Pleistocene climatic fluctuations for range formation and population history of many biota. This is true not only for regions that have been directly affected by glaciation, such as mountain ranges both in Europe and North America or the Arctic (e.g., Brunsfeld et al., 2001; Hewitt, 2001; Abbott and Brochmann, 2003; Dobeš et al., 2004; Schönswetter et al., 2005; Guo et al., 2008), but also for other regions, such as eastern North America (Soltis et al., 2006 and references therein). Pleistocene climatic oscillations also affected the arid habitats of the southwestern United States and adjacent Mexico, which reached their current extent only after the last glacial maximum in a phase of large-scale aridification (McClaran and van Devender, 1995; Bousman, 1998; Metcalfe et al., 2000; Musgrove et al., 2001; Holmgren et al., 2007). Prior to this aridification, drought-adapted species persisted in one or more distinct refugia, from where they reached their current distribution after range expansion within the last 12,000 years (van Devender, 1990; Holmgren et al., 2007). Hence, genetic patterns in those species are expected to reflect both phylogeographic structure due to isolation in refugia and population expansion and secondary contact due to Holocene range expansions (Hewitt, 2001, 2004). In contrast to animals (Taulman and Robbins, 1996;

* Corresponding author. Fax: +43 1 4277 9541.
E-mail addresses: carolin.anna.rebernig@univie.ac.at (C.A. Rebernig), hanna.schneeweiss@univie.ac.at (H. Weiss-Schneeweiss), gerald.schneeweiss@univie.ac.at (G.M. Schneeweiss), peter.schoenswetter@univie.ac.at (P. Schönswetter), renate.obermayer@univie.ac.at (R. Obermayer), vrios@ibiologia.unam.mx (J.L. Villaseñor), tod.stuessy@univie.ac.at (T.F. Stuessy).

1055-7903/$ - see front matter © 2009 Elsevier Inc. All rights reserved.
doi:10.1016/j.ympev.2009.10.010

Pook et al., 2000; Riddle and Hafner, 2006 and references therein; Castoe et al., 2007; Waltari et al., 2007), these predictions have been rarely tested in plants. The few available studies do show evidence for Pleistocene refugia and population expansion (Nason et al., 2002; Clark-Tapia and Molina-Freaner, 2003; Fehlberg and Ranker, 2009; Garrick et al., 2009; Sosa et al., 2009), but they also highlight that each species has its idiosyncratic phylogeographic history. For instance, in the Sonoran Desert *Lophocereus schottii* (Cactaceae) expanded northwards from a single refugium in the southern Baja California peninsula region and shows strong signal of vicariance between peninsular and mainland populations (Nason et al., 2002), whereas *Euphorbia lomelii* expanded southwards and the mainland populations likely originated after long distance dispersal across the Sea of Cortez from the Baja California peninsula (Garrick et al., 2009).

A major force in plant evolution and diversification is polyploidy (Ramsey and Schemske, 1998, 2002; Wendel, 2000). It is estimated that at least 70% (but probably all higher plants, with the possible exception of *Amborella*) have undergone at least one round of polyploidization in their history (Leitch and Bennett, 1997, 2004; Leitch and Leitch, 2008; Soltis et al., 2009). Polyploidy is recognized as an important mode of diversification by, for instance, promoting adaptation to new ecological niches or conferring reproductive isolation, which may eventually lead to speciation (Otto and Whitton, 2000). While allopolyploids may differ conspicuously from their diploid progenitors in morphology and physiology, autopolyploids are often more difficult to distinguish on the basis of morphology alone (Levin, 1983, 2002). Autopolyploids often co-exist within diploid parental populations (Husband, 2004; Suda et al., 2007), and despite several studies on rates and mechanisms of polyploid origin and their establishment relative to their progenitors (Jackson and Hauber, 1982; Felber, 1991; Husband and Schemske, 2000; Baack, 2005; Ramsey et al., 2008), the factors involved in new cytotype formation and particularly in establishment remain insufficiently understood (Baack and Stanton, 2005). In a phylogeographic context, polyploidy can provide information on the direction of the evolution of populations because the evolution of polyploids from lower ploidy levels is largely unidirectional (Meyers and Levin, 2006).

A good system to investigate range dynamics in conjunction with polyploid evolution in xeric habitats is series *Leucantha* of the genus *Melampodium* (Asteraceae). This phylogenetically distinct complex (Blöch et al., 2009) includes three species, with a collective distributional area in the southwestern USA and northern Mexico (ranging from the Sonoran via the Chihuahuan Desert to the Southern and Tamaulipan Plains; Stuessy, 1971a). Here, we focus on *M. cinereum*, which is restricted to the Tamaulipan mezquital ecoregion (Olson et al., 2001), characterized by grass- and thorny scrublands, and the eastern margins of the Chihuahuan Desert (Stuessy, 1971a, 1972). Within its range, *M. cinereum* shows extensive geographically structured morphological and cytological variation (Stuessy, 1971a, 1972). Stuessy et al. (2004) hypothesized that this pronounced geographical structure might be connected to major climatic changes taking place in this region during the Pleistocene, especially during the last glacial maximum (Holmgren et al., 2007).

Our general aim is to elucidate the phylogeographical history of *M. cinereum*, also in the context of polyploid evolution. To this end, we generated amplified fragment length polymorphism (AFLP) and plastid DNA sequence data from 25 populations covering the entire distribution of the species, determined the ploidy level of most individuals with flow-cytometry, and analyzed those data using, among others, a coalescent-based Bayesian approach for hypothesis testing and molecular dating. Specifically, we want to test: (1) whether the current grouping based on morphology is congruent with the genetic population structure likely determined by isolation in different refugia; (2) whether and how this xerophilous species responded to the massive aridification after the last glacial maximum (Holmgren et al., 2007); and (3) whether polyploids originated once, as suggested by their narrow distribution parapatric to diploids, or recurrently.

2. Materials and methods

2.1. Study species

Melampodium cinereum is a drought-tolerant, low-growing, perennial subshrub with white-rayed flowering heads distributed in xeric habitats of southern Texas and adjacent Mexico (Fig. 1). It is morphologically most easily distinguishable from its closest relatives *M. leucanthum* and *M. argophyllum* by the outer phyllaries being connate only one-fourth of their length (Stuessy, 1972). Based on morphological variation concerning size of flower heads, shape of leaves, and indumentum of leaves and stems (length and density of hairs), three varieties *cinereum*, *hirtellum* and *ramosissimum* have been distinguished. Although largely separated geographically (Fig. 1), the ranges of the three varieties overlap near the Rio Grande valley in southern Texas, where the occurrence of morphological intermediates has been hypothesized to be the result of hybridization (Stuessy, 1972). Flowering time spans several months and, despite some differences, flowering times of the varieties overlap at least five months (Stuessy, 1972). Based on the chromosome base number $x = 10$ (Weiss-Schneeweiss et al., 2009), the species comprises morphologically indistinguishable diploid and tetraploid cytotypes (with occasional tri-, penta- or hexaploids; Stuessy et al., 2004; Obermayer et al., unpublished data), especially in var. *cinereum*, where tetraploids are frequent and occupy a distinct distributional area in eastern Texas to the exclusion of diploids (Stuessy et al., 2004).

2.2. Plant material

Plant material from 113 individuals was collected in 25 populations of *M. cinereum* covering the whole range of the species (Fig. 1): 17 of var. *cinereum* (pops. 1–17), six of var. *hirtellum* (pops. 18–23) and two of var. *ramosissimum* (pops. 24 and 25; Table 1). Samples were dried and stored in silica gel until DNA isolation. Vouchers are deposited in the herbarium of the University of Vienna (WU).

2.3. Ploidy level determination

DNA ploidy levels (Suda et al., 2006) were determined on a Partec PAII flow cytometer equipped with a mercury lamp (Partec, Münster, Germany), using DAPI stained DNA of silica-dried leaf material following the method of Suda and Trávníček (2006) except for using only half of the amount of Otto II buffer. Buffer composition was further optimized by adding ascorbic acid and polyvinylpyrrolidone (PVP40) to final concentrations of 0.586 mg/ml and 16.666 mg/ml, respectively (Bharathan et al., 1994). As internal reference size standard, fresh leaves of *Glycine max* 'Merlin' (1C = 1.134 pg; Greilhuber and Obermayer, 1997) were co-analyzed with the test material. A few individuals (7%) could not be analyzed due to the poor quality of the leaf material. The correct interpretation of DNA ploidy levels was confirmed by chromosome numbers determined for selected individuals using standard Feulgen staining as described by Weiss-Schneeweiss et al. (2007).

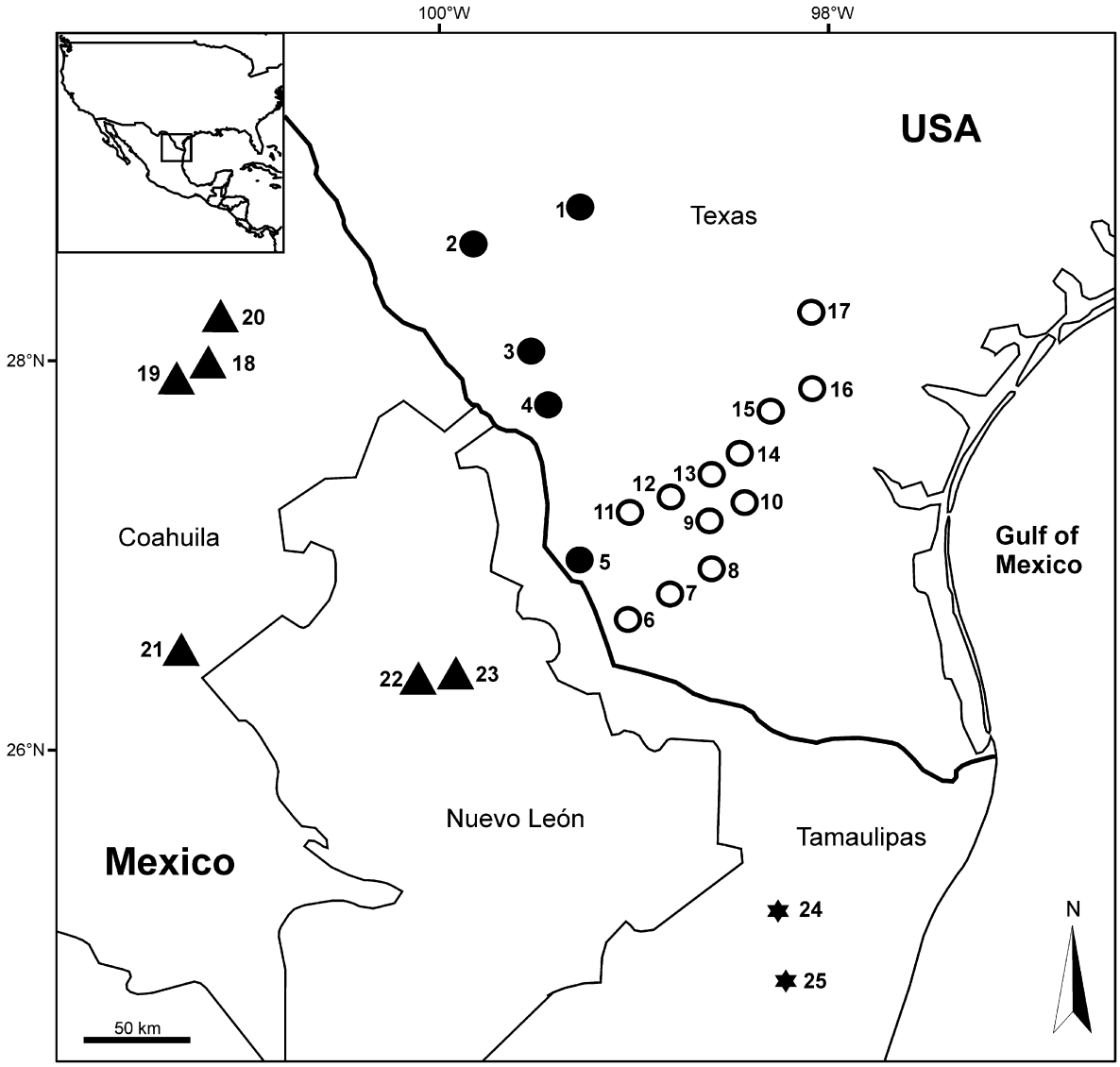

Fig. 1. Distribution map of analyzed populations of *M. cinereum* var. *cinereum* (closed circles, diploids; open circles, tetraploids), var. *hirtellum* (triangles) and var. *ramosissimum* (stars). The collection area represents the entire distribution of *M. cinereum*.

2.4. Molecular methods

Total genomic DNA was extracted from c. 0.5 g of dried tissue following the modified CTAB-protocol of Tel-Zur et al. (1999). Prior to extraction with high-salt CTAB buffer the ground tissue was washed five times with a wash buffer containing sorbitol to remove polysaccharides. DNA concentration of the extracts was quantified photometrically using a DyNA Quant 200 Fluorometer (Amersham Bio sciences, Piscataway, NJ, USA).

AFLP fingerprint profiles were generated for 2–6 individuals per population (Table 1) totaling 113 individuals plus 6.25% replicated samples following the protocol described in Dixon et al. (2008). Two negative controls were performed in each restriction/ligation and PCR run. After screening of 33 selective primer combinations with three or four selective nucleotides the following six primer combinations were selected (fluorescent dyes in parentheses): EcoRI-ACA/MseI-CAT (FAM), EcoRI-ACG/MseI-CAA (VIC), EcoRI-ACC/MseI-CAG (NED), EcoRI-ACT/MseI-CAC (FAM), EcoRI-AGG/MseI-CAA (VIC), EcoRI-AGG/MseI-CAC (NED). The selective PCR products were purified using Sephadex G-50 Superfine according to the manufacturer's instructions (GE Healthcare Bio-Sciences, Uppsala, Sweden). The amplification products were run on a 3130xl Genetic Analyzer capillary sequencer (Applied Biosystems, Foster City, CA, USA) using GeneScan 500 ROX as the internal size standard (Applied Biosystems). Raw data were aligned with the internal size standard using ABI Prism GeneScan 3.7 (Applied Biosystems) and the GeneScan files were imported into Genographer 1.6.0 (available from http://hordeum.oscs.montana.edu/genographer) for scoring. Unambiguous bands in the size range of 100–500 bp were scored, and the results were exported as a presence/absence matrix. We explicitly did not score shorter fragments due to the higher frequency of non-homologous fragments in this size class (Vekemans et al., 2002). Non-reproducible bands identified by comparisons among replicated individuals were excluded from all further analyses.

The following four non-coding chloroplast DNA spacer regions were amplified for 3–4 individuals per population (Table 1) totaling 77 individuals: *psb*A-*trn*H, *ndh*F-*rpl*32, *rpl*32-*trn*L, and *trn*Q-*rps*16. The PCR mixture for the amplification contained 1× Reddy Mix PCR Master Mix (including 2.5 mM $MgCl_2$; ABgene, Epsom, UK), 0.5 μM each of forward and reverse primers (Sang et al., 1997, and Tate and Simpson, 2003, for *psb*A-*trn*H; Shaw et al.,

Table 1
Sampling location coordinates, voucher information (collection numbers of Stuessy et al.), number of analyzed individuals, AFLP data descriptives, DNA ploidy levels and GenBank accession numbers.

Variety and population number	Location (voucher)[a]	Sample size AFLP/cpDNA	$Frag_{tot}$[b]	$Frag_{poly}$[c]	$Frag_{priv}$[d]	AWD ± SD[e]	Ploidy	GenBank Accession Numbers[f]
cinereum								
1	T: N 28°46.313' W 99°16'43.5" (18688)	4/3	287	59.2	8	0.109 ± 0.223	2*x*	FJ456097–FJ456099; FJ456020–FJ456022; FJ456174–FJ456176; FJ456251–FJ456253
2	T: N 28°36.492' W 99°50'27.1" (18689)	5/3	262	66.8	5	0.099 ± 0.202	2*x*	FJ456100–FJ456102; FJ456023–FJ456025; FJ456177–FJ456179; FJ456254–FJ45656
3	T: N 28°02.119' W 99°31'42.7" (18690)	5/3	264	64.0	2	0.105 ± 0.206	2*x*	FJ456103–FJ456105; FJ456026–FJ45628; FJ456180–FJ456182; FJ456257–FJ456259
4	T: N 27°46.850' W 99°27'03.7" (18691)	2/3	238	39.9	1	––	2*x*	FJ456106–FJ456108; FJ456029–FJ456031; FJ456183–FJ456185; FJ456260–FJ456262
5	T: N 26°53.417' W 99°15'42.1" (18693)	2/3	238	38.2	3	––	2*x*	FJ456109–FJ456111; FJ456032–FJ456034; FJ456186–FJ456188; FJ456263–FJ456265
6	T: N 26°41.812' W 99°06'33.5" (18694)	5/3	301	61.5	2	0.105 ± 0.207	4*x*	FJ456112–FJ456114; FJ456035–FJ456037; FJ456189–FJ456191; FJ456266–FJ456268
7	T: N 26°48.167' W 98°51'18.2" (18697)	5/3	288	60.4	0	0.095 ± 0.195	4*x*	FJ456115–FJ456117; FJ456038–FJ456040; FJ456192–FJ456194; FJ456269–FJ456271
8	T: N 26°56.489' W 98°37'09.0" (18698)	5/3	300	62.0	5	0.105 ± 0.207	4*x*	FJ456118–FJ456120; FJ456041–FJ456043; FJ456195–FJ456197; FJ456272–FJ456274
9	T: N 27°11.720' W 98°37'18.3" (18699)	3/3	284	41.9	2	––	4*x*	FJ456121–FJ456123; FJ456044–FJ456046; FJ456198–FJ456200; FJ456275–FJ456277
10	T: N 27°15.866' W 98°29'10.3" (18700)	5/3	304	65.7	3	0.111 ± 0.209	4*x*	FJ456124–FJ456126; FJ456047–FJ456049; FJ456201–FJ456203; FJ456278–FJ456280
11	T: N 27°16.677' W 98°44'01.4" (18701)	5/3	292	57.9	0	0.095 ± 0.199	4*x*	FJ456127–FJ456129; FJ456050–FJ456052; FJ456204–FJ456206; FJ456281–FJ456283
12	T: N 27°13.942' W 98°56'02.3" (18702)	5/3	329	63.5	3	0.118 ± 0.216	4*x*	FJ456130–FJ456132; FJ456053–FJ456055; FJ456207–FJ456209; FJ456284–FJ456286
13	T: N 27°24.270' W 98°34'34.8' (18704)	4/3	257	54.9	0	0.087 ± 0.201	4*x*	FJ456133–FJ456135; FJ456056–FJ456058; FJ456210–FJ456212; FJ456287–FJ456289
14	T: N 27°30.766' W 98°28'50.2" (18705)	4/4	274	63.5	1	0.108 ± 0.218	4*x*	FJ456136–FJ456139; FJ456059–FJ456062; FJ456213–FJ456216; FJ456290–FJ456293
15	T: N 27°43.952' W 98°15'47.3" (18706)	4/3	298	54.4	0	0.103 ± 0.210	4*x*	FJ456140–FJ456142; FJ456063–FJ456065; FJ456217–FJ456219; FJ456294–FJ456296
16	T: N 27°52.192' W 98°05'15.4" (18707)	5/3	302	59.3	0	0.098 ± 0.198	4*x*	FJ456143–FJ456145; FJ456066–FJ456068; FJ456220–FJ456222; FJ456297–FJ456299
17	T: N 28°14.514' W 98°06'22.3" (18708)	4/3	258	55.8	2	0.090 ± 0.0234	4*x*	FJ456146–FJ456148; FJ456069–FJ456071; FJ456223–FJ456225; FJ456300–FJ456301
	Mean	4.2/3.1	266.9	56.99	2.18	0.102 ± 0.0260		
hirtellum								
18	M: N 27°56'44.8" W 101°15'24.3" (19054)	5/4	271	59.4	13	0.090 ± 0.194	2*x*	FJ456149–FJ456152; FJ456072–FJ456075; FJ456226–FJ456229; FJ456303–FJ456306
19	M: N 27°54'10.4" W 101°20'33.8" (19055)	5/3	279	64.5	4	0.101 ± 0.203	2*x*	FJ456153–FJ456155; FJ456076–FJ456078; FJ456230–FJ456232; FJ456307–FJ456309
20	M: N 28°11'36.0" W 101°04'18.7" (19057)	5/3	266	57.5	4	0.083 ± 0.184	2*x*	FJ456156–FJ456158; FJ456079–FJ456081; FJ456233–FJ456235; FJ456310–FJ456312
21	M: N 26°30'31.4" W 101°21'06.4" (19058)	5/3	299	57.9	17	0.094 ± 0.199	2*x*	FJ456159–FJ456161; FJ456082–FJ456084; FJ456236–FJ456238; FJ456313–FJ456315
22	M: N 26°21'56.7" W 100°07'22.6" (19061)	6/3	268	77.6	10	0.105 ± 0.194	2*x*	FJ456162–FJ456164; FJ456085–FJ456087; FJ456239–FJ456241; FJ456316–FJ456318
23	M: N 26°37'34.2" W 100°01'32.6" (19062)	5/3	211	80.1	4	0.095 ± 0.198	2*x*	FJ456165–FJ456167; FJ456088–FJ456090; FJ456242–FJ456244; FJ456319–FJ456321
	Mean	5.2/3.2	265.7	66.2	8.67	0.095 ± 0.009		
ramosissimum								
24	M: N 25°10'48.4" W 98°11'56.1" (19063)	5/3	197	63.5	2	0.082 ± 0.202	2*x*	FJ456168–FJ456170; FJ456091–FJ456093; FJ456245–FJ456247; FJ456322–FJ456324
25	M: N 24°48'59.3" W 98°11'00.6" (19065)	5/3	272	63.6	12	0.099 ± 0.203	2*x*	FJ456171–FJ456173; FJ456094–FJ456096; FJ456248–FJ456250; FJ456325–FJ456327
	Mean	5.0/3.0	234.5	63.6	7.00	0.091 ± 0.012		

[a] M, Mexico; T, Texas.
[b] Total number of AFLP fragments.
[c] Percentage of polymorphic bands.
[d] Number of private fragments.
[e] Average differences within populations ± standard deviation calculated for populations with more than three individuals.
[f] *psb*A-*trn*H; *ndh*F-*rpL*32; *rpL*32-*trn*L; *trn*Q-*rps*16.

2007, for all others), 0.8 μg/μl BSA (bovine serum albumin; Promega, Madison, WI, USA) and c. 50 ng of DNA template. Amplification was performed on a T-CY thermocycler (Creacon Technologies, Emmen, The Netherlands) under the following conditions (those for *psb*A-*trn*H in parentheses): 3 min at 95 °C (5 min at 94 °C) followed by 38 (36) cycles each of 1 min (30 s) denaturation at 95 °C (94 °C), 1 min (30 s) annealing at 50 °C (52 °C), and 4 min (1 min) elongation at 65 °C (72 °C) followed by a final elongation phase of 5 min (10 min) at 65 °C (72 °C). PCR products were purified using *E. coli* Exonuclease I and Calf Intestine Alkaline Phos-

phate (CIAP; MBI-Fermentas, St. Leon-Rot, Germany) according to the manufacturer's instructions. Cycle sequencing was performed using Big Dye™ Terminator v3.1 Ready Reaction Mix (Applied Biosystems) using the following cycling conditions: 38 cycles of 10 s at 96 °C, 25 s at 50 °C, 4 min at 60 °C. All DNA regions were sequenced in both directions. The samples were run on a 3130xl Genetic Analyzer capillary sequencer (Applied Biosystems). Sequences were assembled using SeqMan II (DNAStar Inc., Madison, WI, USA) and manually aligned using BioEdit 7.0 (Hall, 1999). Sequences are deposited in GenBank (Accession Numbers FJ456020–FJ456327; Table 1).

2.5. Data analysis

2.5.1. AFLPs

AFLP data descriptives include the total number of fragments ($Frag_{tot}$), the percentage of polymorphic fragments ($Frag_{poly}$), the number of private fragments ($Frag_{priv}$), and the index of average differences within populations (AWD; Kosman, 2003) calculated for populations with more than three individuals in Arlequin 3.10 (Excoffier et al., 2005). Both a non-hierarchical and a three-level hierarchical AMOVA using the five groups suggested by BAPS and the four groups suggested by Structure and by Barrier (see Section 3.2, AFLP Results) were conducted in Arlequin 3.10, and the significance of variance components was estimated from 1000 permutations. Genetic relationships among individuals were analyzed using the neighbor-net method implemented in SplitsTree 4.8 (Huson and Bryant, 2006) based on Nei–Li distances (Nei and Li, 1979) calculated with FAMD 1.108 (Schlüter and Harris, 2006). Bootstrap support values were calculated with Treecon 1.3 (van de Peer and de Wachter, 1994) using 2000 replicates.

Genetically homogeneous groups were identified using genetic mixture analysis. The appropriate number of groups (K) and the most likely assignment of each individual to a certain group without a priori information about population structure were estimated using the programs Structure 2.2 (Pritchard et al., 2000) and BAPS 3.2 (Corander et al., 2006). For Structure, models with uncorrelated allele frequencies with or without admixture were used. K values ranging from 1 to 10 were tested, employing for each K 10 independent runs with 550,000 MCMC generations (the first 50,000 were discarded as burn-in, which was well after the chain had reached stationarity). The optimal number of clusters was determined from the similarity coefficients as defined by Rosenberg et al. (2002) as implemented in the R-script Structure 2.1-SUM (Ehrich, 2006). Results of the replicated runs were averaged using CLUMPP 1.1.1 (Jakobsson and Rosenberg, 2007). In contrast to Structure, BAPS, which uses stochastic optimization (Corander et al., 2006) instead of MCMC, treats K as a variable to estimate and gives a list of the best partitioning and their likelihood scores. For BAPS mixture analysis an upper bound of populations (K) of 25 was used with 10 replicates for each K. Admixture coefficients were estimated using 10,000 iterations, and the significance of these coefficients was estimated by employing the simulation strategy described by Corander and Marttinen (2006) with 15 iterations of 50 reference individuals and a minimum population size of 3. In order to assess the influence of including both diploid and tetraploid individuals, both Structure and BAPS were also run with diploids only.

In order to identify genetic breaks we used BARRIER 2.2 (Manni et al., 2004), which employs Monmonier's maximum distance algorithm to find zones of largest genetic distances. We used net average Nei–Li distances between populations calculated in MEGA 4 (Tamura et al., 2007) as genetic distances. Using other population distance measures, such as chord distances from allele frequencies estimated using a Bayesian method with non-uniform priors (Zhivotovsky, 1999) as implemented in FAMD 1.108 (Schlüter and Harris, 2006), gave congruent results (data not shown). Robustness of computed barriers was assessed via a bootstrap analysis using 100 resampled bootstrap matrices. The number of barriers was set to 4 (number of groups – 1) in accordance with the BAPS results (see Section 3.2, AFLP results). In order to test whether genetic breaks are the result of isolation in separate refugia (vicariance) or simply a result of limited dispersal (isolation by distance), we regressed pairwise genetic distances (in percent) between populations belonging to different phylogroups against their pairwise geographic distances (in km, calculated using the Geographic Distance Matrix Generator 1.2.3: Ersts, 2009) using reduced major axis regression implemented in RMA for Java 1.21 (Bohonak and van der Linde, 2004). A positive relationship between genetic and geographic distances is expected under the isolation by distance model, whereas the absence of such a relationship is consistent with the vicariance model. Regression parameters were estimated using one-delete jackknife, and their confidence intervals (C.I.) were determined using bootstrapping over 10,000 replicates.

The most likely origins of the tetraploid individuals of *M. cinereum* var. *cinereum* were determined using the default settings of the assignment test implemented in AFLPOP 1.1 (Duchesne and Bernatchez, 2002) considering the diploid populations of all varieties as potential source populations. Allocation was tested using three different levels (0, 1 or 2) of minimal log-likelihood differences (as recommended by Duchesne and Bernatchez, 2002) with frequency values of zero replaced by 1/(sample size + 1).

2.5.2. cp DNA

Prior to all analyses, inversions in the plastid sequence data were manually reversed, as these would introduce substitutional mutations, which in fact are the result of structural mutations (Löhne and Borsch, 2005). Both non-hierarchical and hierarchical AMOVAs using the same groups as for the AFLP analysis were conducted as described above. A network was constructed using statistical parsimony as implemented in TCS (Clement et al., 2000) with the connection limit set to 95% and gaps treated as fifth character. For the TCS analysis, indels longer than 1 bp and inversions were recoded as single characters (effectively by reducing those regions to single base pair columns allowing those structural mutations to be counted as single base pair mutations only) and mononucleotide repeats were removed due to their high degree of homoplasy (Ingvarsson et al., 2003).

Reconstruction of the demographic history and molecular dating were conducted using BEAST 1.4.8 (Drummond and Rambaut, 2007) on the University of Vienna computer cluster (Schrödinger III, http://www.univie.ac.at/ZID/schroedinger/). As the plastid genome behaves as a single linkage group and our data consisted mostly of non-coding spacer and intron regions, we applied a single GTR+Γ model to all data. Although the AIC criterion implemented in ModelTest 3.6 (Posada and Crandall, 1998) suggested models additionally including a parameter describing the proportion of invariable sites, we subsumed this in the gamma distribution modeling rate heterogeneity across sites, using six rate categories instead of the default four. For all substitution model parameters, uniform priors (0, 100) were used. Since a strict clock model was rejected (Bayes factors [see below] <– 30; data not shown), rate evolution was modeled in a relaxed clock framework using a lognormal distribution (Drummond et al., 2006) with uniform distributions for mean and standard deviation of 0–100 and 0–10, respectively. Due to the lack of external calibrations, we used a strong prior on the substitution rate. Based on estimates of synonymous substitution rates for the plastid *mat*K gene in *Fagopyrum* (Polygonaceae) and on estimates of substitution rates for the *trn*T-*trn*L intergenic spacer in Agavaceae of 4.0×10^{-9} substitutions per site and year (Yamane et al., 2003; Smith et al., 2008), we modeled

the substitution rate with a normal distribution with mean and standard deviation of 4.0×10^{-3} and 2.0×10^{-3} substitutions per site and million years, respectively. After initial analyses, the root of the tree was constrained to be maximally 10 million years old. We compared several different demographic models: the Bayesian skyline plot (Drummond et al., 2005) as the most general demographic model, using four different group intervals ($m = 10$, 20, 30, 40); a model of constant population size as the simplest demographic history; an exponential growth model born from the hypothesis that the aridification at the end of the last glacial maximum caused an extension of the distribution of the xerophilous *M. cinereum*; and a two-epoch model, where a phase of constant population size is followed by a phase of logistic growth, thus aiming at describing the changes in effective population sizes inferred from the Bayesian skyline plot (see Section 3.3) with a less parameterized model. The BEAST input files (txt-files), which also include the exact parameterization of the demographic models, are available as Supplementary online material. For all demographic models used we tested whether polyploid populations of *M. cinereum* var. *cinereum* originated once (i.e., constitute a monophyletic group) as suggested by their compact distribution parapatric to that of the diploids. All hypothesis testing employed Bayes factors (BF), which are the Bayesian analog of the likelihood ratio test (Suchard et al., 2001, 2005). Marginal likelihoods (including their Monte Carlo error: Suchard et al., 2003; Redelings and Suchard, 2005) and BFs were calculated with Tracer 1.4 (available from http://evolve.zoo.ox.ac.uk/). As test statistic we used the widely applied $2 \times \ln BF$, considering $2 \times \ln BF_{\text{model 1 vs. model 2}} > 10$ as strong support for model 1 (Kass and Raftery, 1995).

As alternative approaches to test for population expansion we used neutrality tests (Tajima, 1996; Fu, 1997) and mismatch distribution (the distribution of pairwise differences among individuals; Rogers and Harpending, 1992) calculated in Arlequin 3.10 (Excoffier et al., 2005). Specifically, significantly negative Tajima's D (Tajima, 1996) and Fu's F_S (Fu, 1997), whose significances were assessed by 10,000 samples simulated under a model of constant population size, indicate population expansion. Under a model of population expansion, the mismatch distribution is expected to be unimodal (Rogers and Harpending, 1992). Agreement between the observed and the expected distribution under a sudden-expansion model was tested via the sum of squared differences, which, if significant at $P \leqslant 0.05$, indicates deviation from the expansion model (Schneider and Excoffier, 1999). Significance was assessed via a non-parametric bootstrapping procedure with 10,000 replicates. Using the moment estimator τ, which was derived from both a model of population expansion and one of spatial expansion (Excoffier, 2004) from the mismatch distribution, the absolute time of expansion (t) was derived via the formula $t = \tau/2\,\mu$, where μ is the mutation rate per gene region and per generation (Rogers and Harpending, 1992). We used substitution rates of 4×10^{-9} substitutions per site and year, as for the BEAST analyses (see above), and assumed generation times of five years to estimate u as 6.57×10^{-5} substitutions per gene and generation. Confidence intervals for τ were estimated via a bootstrap procedure employing 10,000 replicates (Schneider and Excoffier, 1999).

3. Results

3.1. Ploidy level

Analyses of DNA ploidy level of most individuals used for the molecular analyses showed the presence of two distinct classes of nuclear DNA amount (Fig. S1, Table S1, both available as Supplementary online material), which, as confirmed by chromosome counts (Table S1), correspond to diploid and tetraploid cytotypes. Tetraploids were found only in var. *cinereum* (pops. 6–17). Intrapopulational cytotype mixture of diploids and tetraploids was neither detected in individuals analyzed here nor in a larger data set (450 individuals) including many more individuals per population (Obermayer et al., unpublished data). Neither the single triploid individual in an otherwise diploid population (pop. 21) nor the few penta- and hexaploid individuals encountered in otherwise tetraploid populations (pops. 6, 8, 17; Obermayer et al., unpublished data) were included in the molecular analyses.

3.2. AFLPS

The six AFLP primer combinations chosen for the analysis generated 871 unambiguously scorable fragments, ranging in size from 100–500 bp: EcoRI-ACA/MseI-CAT (FAM): 143 fragments; EcoRI-ACG/MseI-CAA (VIC): 175 fragments; EcoRI-ACC/MseI-CAG (NED): 134 fragments; EcoRI-ACT/MseI-CAC (FAM): 149 fragments; EcoRI-AGG/MseI-CAA (VIC): 133 fragments; EcoRI-AGG/MseI-CAC (NED): 137 fragments. All 113 individuals investigated had a unique AFLP profile. The error rate (Bonin et al., 2004) based on phenotypic comparisons among replicated individuals amounted to 4%.

The distribution of the genetic diversity estimated with AWD ranged from 0.082 ± 0.202 (pop. 24) to 0.118 ± 0.216 (pop. 12) and did not show any apparent geographic pattern (Table 1). The highest diversity was found in var. *cinereum* (0.102 ± 0.026), followed by var. *hirtellum* (0.095 ± 0.009) and var. *ramosissimum* (0.091 ± 0.012; Table 1). Non-hierarchical AMOVA of the AFLP data of all 25 populations indicated that 56.88% of the total variation was apportioned within populations and 43.12% among populations. In a hierarchical AMOVA based on the five groups suggested by BAPS (see below), 25.62% of the variation was found among groups, while 21.71% of the variation was among populations within groups and 52.67% within populations (analyses with four groups, as suggested by Structure and by Barrier, gave nearly identical results, Table 2).

The neighbor-net network revealed two major groups separated by a well-supported (bootstrap [BS] 100%, obtained from a neighbor joining analysis) split (Fig. 2). The first group comprised diploid (A, pops. 1–5) and tetraploid accessions of var. *cinereum* (B, pops. 6–7; C, pops. 8–17) and the western populations of var. *hirtellum* (D, pops. 18–21). While the diploid groups A and D were well-supported (BS 100%), the tetraploid ones had no common split (Fig. 2). The second group consisted of a group including two eastern populations of var. *hirtellum* (E, pops. 22–23; BS 100%) and the populations of var. *ramosissimum* (F, pops. 24–25; BS 100%). All populations were monophyletic. Neighbor-net analyses of populations, using net average Nei–Li distances, gave very similar results, with diploid var. *cinereum* (group A) being more clearly separated from a cohesive group of tetraploid var. *cinereum* (group B/C; Fig. S2, available as Supplementary online material).

Non-hierarchical clustering using Structure suggested $K = 4$ clusters as the optimal solution (Fig. 3a; Fig. S3, available as Supplementary online material), irrespective of using an admixture or a no-admixture model. These clusters included (corresponding groups from the neighbor-net analysis given in parentheses) diploid var. *cinereum* (group A), tetraploid var. *cinereum* (groups B and C), western var. *hirtellum* (group D) and eastern var. *hirtellum* plus var. *ramosissimum* (groups E and F). Bayesian clustering using BAPS gave similar results, but the optimal solution assigned eastern var. *hirtellum* and var. *ramosissimum* to separate clusters (Fig. 3b). Excluding the tetraploid individuals had no effect on the clustering of diploids (data not shown). The level of admixture between the clusters was generally low. Some admixture was inferred between the clusters of diploid and tetraploid var. *cinereum* and in the cluster of var. *ramosissimum* (Fig. 3).

Table 2
Three-level hierarchical AMOVAs of AFLP and cpDNA data.

Source of variation	df	Sum of squares	Variance components	Variation (%)	Φ_{ST}
AFLP					
5 groups[a]					0.4733
Among groups	4	2121.88	21.02	25.62	
Among populations	20	2432.86	17.81	21.71	
Within populations	87	3761.05	43.23	52.67	
4 groups[b]					0.4698
Among groups	3	1838.70	18.90	23.18	
Among populations	21	2716.06	19.40	23.80	
Within populations	87	3761.05	43.23	53.02	
4 groups[c]					0.4953
Among groups	3	1762.82	22.03	25.73	
Among populations	21	2791.93	20.38	23.80	
Within populations	87	3761.05	43.23	50.47	
cpDNA					
5 groups[a]					0.6321
Among groups	4	97.81	0.67	8.78$^{n.s.}$	
Among populations	20	311.42	4.15	54.43	
Within populations	52	145.75	2.80	36.79	
4 groups[b]					0.6325
Among groups	3	82.15	0.67	8.80$^{n.s.}$	
Among populations	21	327.09	4.15	54.45	
Within populations	52	145.75	2.80	36.75	
4 groups[c]					0.6308
Among groups	3	58.54	0.54	8.79$^{n.s.}$	
Among populations	21	262.50	3.33	54.29	
Within populations	52	117.67	2.26	36.92	

[a] Groups according to BAPS.
[b] Groups according to Structure.
[c] Groups according to Barrier.

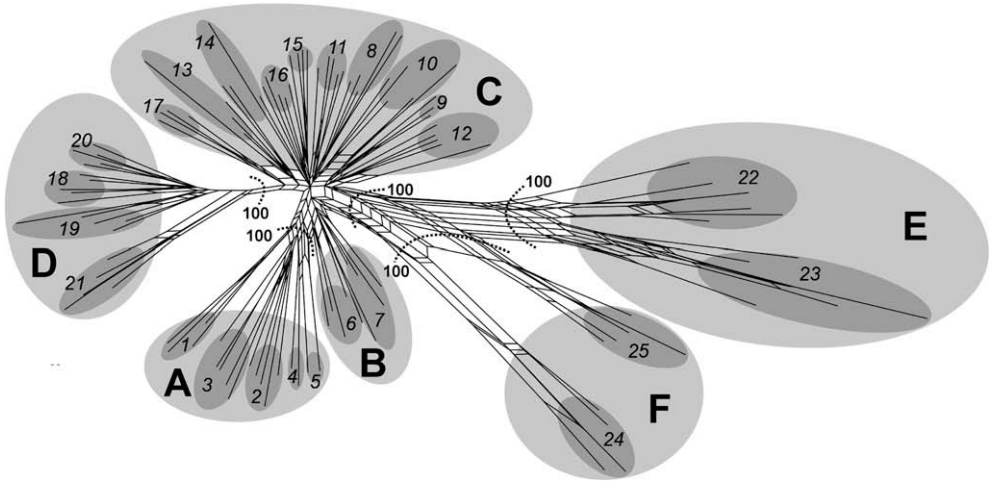

Fig. 2. Neighbor-net for the AFLP data using Nei-Li distances. The circumscription of the groups A–F (A = diploid var. *cinereum*; B, C = tetraploid var. *cinereum*; D = western var. *hirtellum*; E = eastern var. *hirtellum*; F = var. *ramosissimum*) is indicated. Numbers in italics refer to population numbers (Fig. 1, Table 1), numbers in normal font are bootstrap values from a neighbor joining analysis.

The strongest genetic break identified with Barrier was the one separating eastern var. *hirtellum* from the remaining populations, followed by the one separating var. *ramosissimum* from var. *cinereum* and western var. *hirtellum*, the latter being separated by the third break (Fig. 4). Whereas these barriers were very robust (BS 91–100), the position of the fourth barrier separating the two populations of var. *ramosissimum* is only moderately supported (BS 68). There is no continuous barrier separating the diploid populations of var. *cinereum* from the tetraploid ones. There is no significant positive relationship between geographic and genetic distances of populations belonging to different groups (for raw distances: slope ± standard error [SE] −0.0581 ± 0.003 with a 95% C.I. from −0.0643 to −0.0527, r^2 ± SE 0.2724 ± 0.0714 with a 95% C.I. from 0.1536 to 0.4259; for log-transformed distances: slope ± SE −0.2478 ± 0.0163 with a 95% C.I. from −0.2837 to −0.2192, r^2 ± SE 0.2499 ± 0.0564 with a 95% C.I. from 0.1533 to 0.3716), thus rejecting an isolation by distance model.

Genetic assignment tests using a cut-off level of 2 suggested population 3 of var. *cinereum* as the most likely source for the majority of tetraploid individuals (94.45% of the tetraploid individuals). Other inferred source populations included another population of var. *cinereum* (pop. 1; 1.85%) and one of var. *hirtellum* (pop. 19; 1.85%). One tetraploid individual (1.85%) remained unassigned. Using a cut-off level of log-likelihood difference of 1 instead

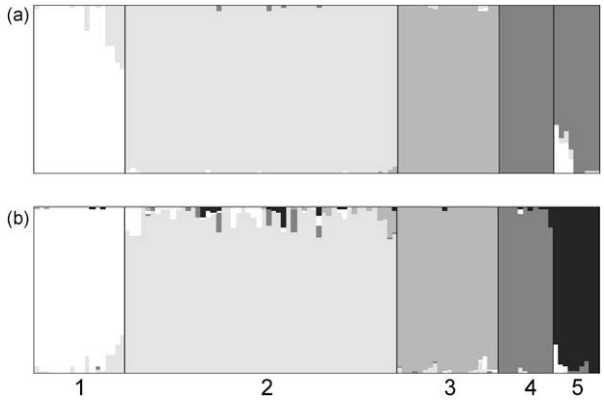

Fig. 3. Population structure estimated with (a) Structure and (b) BAPS. An individual's estimated membership fractions in K clusters are indicated by different shadings. Black lines separate the following groups: 1 = diploid var. *cinereum*; 2 = tetraploid var. *cinereum*; 3 = western var. *hirtellum*; 4 = eastern var. *hirtellum*; 5 = var. *ramosissimum*.

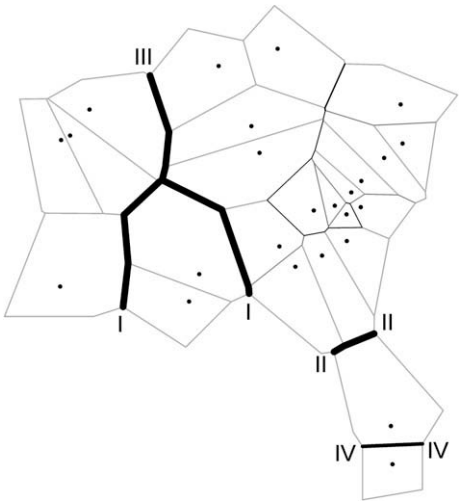

Fig. 4. Location of intraspecific genetic breaks (identified with Barrier), their hierarchical order being indicated by Roman numerals (see text for details). Thickness of lines is proportional to the breaks' robustness summed over 100 bootstrap replicates with four calculated barriers each. Sampled populations are indicated by dots, polygons resulting from Voronoï tessellation are indicated in grey.

of 2 gave almost identical results, only a single individual (1.85%) being assigned to pop. 2 instead of pop. 3. Reducing the cut-off level to 0 resulted in 50 individuals (92.59%) being assigned to pop. 3, a single individual to pop. 1 and three individuals to pop. 19 (5.55%).

3.3. cpDNA data

Approximately 2700 bp of chloroplast DNA were analyzed coming from the regions *psb*A-*trn*H (286–400 bp), *ndh*F-*rpl*32 (957–1069 bp), *rpl*32-*trn*L (713–888 bp), and *trn*Q-*rps*16 (789–814 bp). After conversion of microinversions and character recoding the alignment of 2700 bp included 60 variable characters, of which 52 were parsimony–informative. Hierarchical AMOVA conducted on the cpDNA dataset (five groups as for the AFLP data) assigned 8.78% to variation among groups, though not significant, and 54.43% and 36.79% to variation among and within populations, respectively (again, analysis using four groups as suggested by Structure and by Barrier gave almost identical results, Table 2). The network analysis using statistical parsimony resulted in a single network connecting all 53 haplotypes (Fig. 5). Of these, only 12 were found in more than one individual (two of diploid var. *cinereum*, five of tetraploid var. *cinereum*, three of western var. *hirtellum*, one of eastern var. *hirtellum*, one of var. *ramosissimum*), while the remaining ones were singletons (10 of diploid var. *cinereum*, 19 of tetraploid var. *cinereum*, seven of western var. *hirtellum*, three of eastern var. *hirtellum*, two of var. *ramosissimum*; Fig. 5). The majority of populations (84%) harbored more than one haplotype, which, in several cases, were found in different parts of the network (e.g., pop. 3; Fig. 5). With the exception of haplotypes found in var. *ramosissimum*, those from the other two varieties were highly intermixed (Fig. 5). Although our sampling of haplotypes is clearly incomplete (using the method of Dixon, 2006, the most likely number of haplotypes is 95 with a 95% confidence interval from 75 to 134), it can be expected that denser sampling would further strengthen the pattern of high intrapopulational diversity and heterogeneity.

Bayesian skyline plots with different group intervals (m = 10, 20, 30, 40) gave very similar results with 2 × lnBF not exceeding 2.2 (data not shown), and in the following we present the results with m = 40. The inferred diversification age of *M. cinereum* (mean/median ages and 95% highest posterior density [HPD] intervals are summarized in Table 3) strongly depended on the demographic model used. While a model of constant population size and a two-epoch model had modes between 1.0 and 2.0 Mya with the upper HPD limit > 7 Mya, thus coming close to the *a priori* set limit of 10 Mya, a model of exponential population growth and the Bayesian skyline plot model had modes around 0.5 Mya with the upper HPD limit being < 3 Mya. The Bayesian skyline plot indicated a pronounced increase in effective population size around 0.015 Mya after a long phase of only slightly increasing population size (Fig. 6). Bayes factors, however, favoured the simpler demographic models, the one of constant population size being the best supported (Table 4). Irrespective of demographic model used, the hypothesis of a single origin of polyploids was strongly rejected (2 × lnBF <− 220).

Both neutrality tests and the mismatch distribution supported population or spatial expansion, although not always statistically significant (Tajima's D −0.928, P = 0.173; Fu's F_S −24.398, P < 0.0001; sum of squared deviations under both models 0.0037, P = 0.727 and P = 0.842, respectively, thus not deviating from the expansion model). Based on the moment estimator τ, this expansion is estimated to have occurred 24.0 (5.2–155.8) kyr ago. Using a model of spatial expansion gave very similar results with an expansion time of 21.2 (10.2–208.0) kyr ago.

4. Discussion

Melampodium cinereum is a member of the dry brushland vegetation of Texas and adjacent Mexico and exhibits considerable morphological variation concerning plant height, floret number and density of indumentum. The pronounced geographical structure in the distribution of these phenotypes (Fig. 1), which were recognized as three varieties (Stuessy, 1972), was hypothesized to be connected to major climatic changes taking place in this region during the Pleistocene, especially during the last glacial maximum (Stuessy et al., 2004; Holmgren et al., 2007). AFLP data clearly confirm the presence of well-differentiated genetic lineages within *M. cinereum* (Figs. 2–4). Their number is, however, underestimated by current taxonomy, because var. *hirtellum* includes two lineages, one more closely related to var. *cinereum* (western *hirtellum*) and another to var. *ramosissimum* (eastern *hirtellum*), respectively, than to each other. Furthermore, these lineages are strongly spatially structured (AMOVA-derived F_{ST} = 0.473) and allopatric

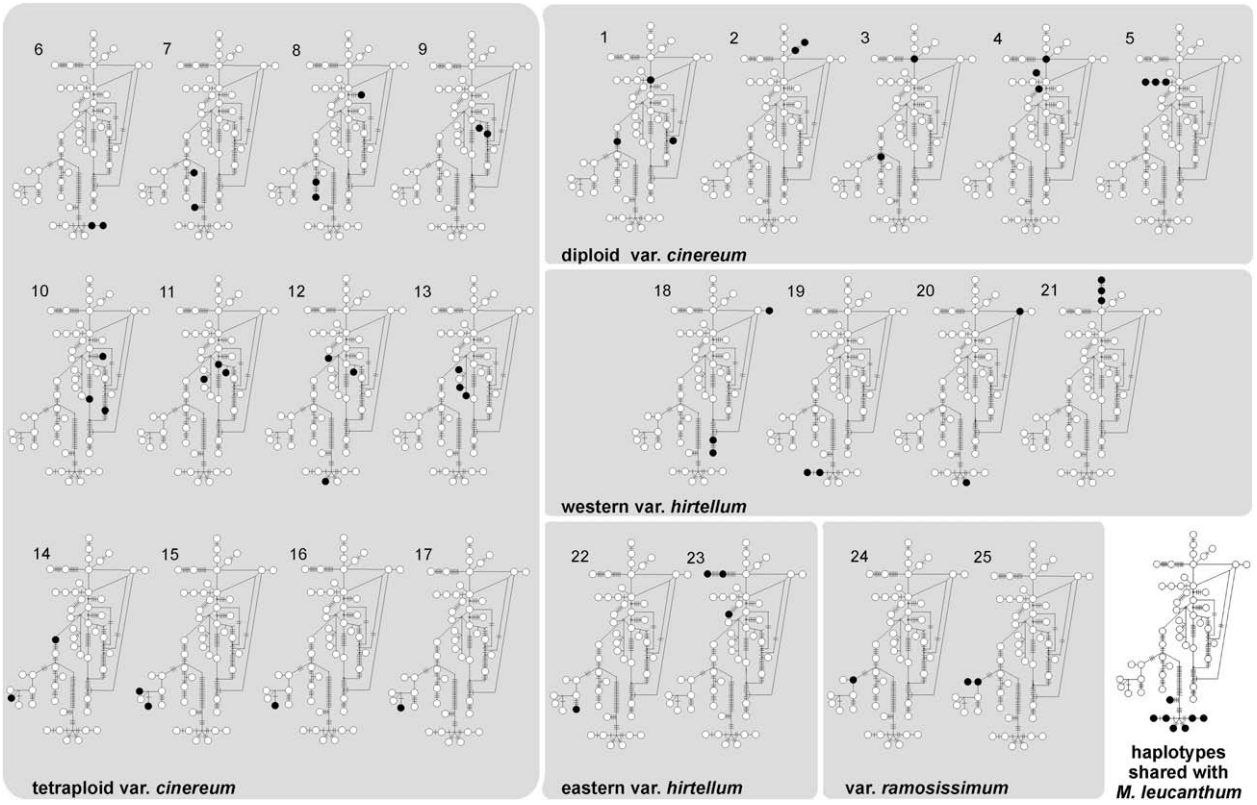

Fig. 5. Haplotype networks of all populations of *M. cinereum* numbered as in Fig. 1 and Table 1. Sampled haplotypes are indicated by circles (black ones indicating those found in the respective populations), unsampled ones by ticks. The last and unnumbered network shows the haplotypes that are shared with *M. leucanthum* (marked in black).

Table 3
Estimates of diversification ages (given as mean/median and, in parentheses, the 95% highest posterior density interval) using a strong prior on the mean substitution rate and four different demographic models ordered by decreasing support (see text for details).

Demographic model	Diversification age (million years)
Constant population size	2.552/1.797 (0.389–7.348)
Exponential population growth	0.933/0.667 (0.164–2.424)
Two-epoch model	4.144/3.547 (0.593–9.143)
Bayesian skyline plot	1.092/0.838 (0.187–2.703)

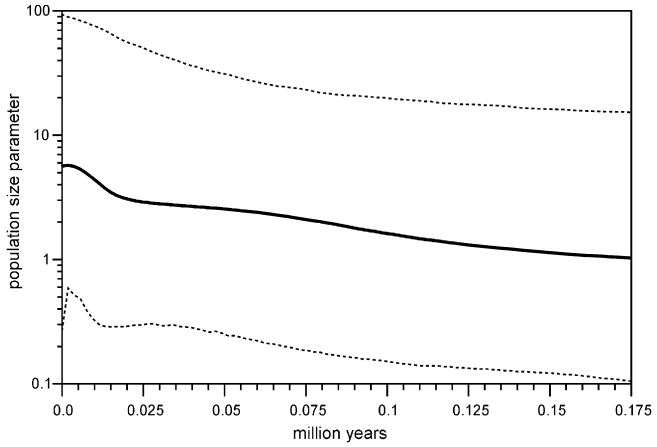

Fig. 6. Bayesian skyline plot of *M. cinereum* showing changes in effective population size (mean and 95% highest posterior density interval) over time. The population size parameter (logarithmic scale) is given as effective population size × generation time in years ($N_e \times \tau$).

(Fig. 1). Nevertheless, as suggested by the presence of hybrids between var. *hirtellum* and var. *cinereum* in the Rio Grande valley (Stuessy, 1972), gene flow among at least some of the genetic lineages appears to occur, albeit the morphological assessment of hybrid individuals requires corroboration from molecular data.

There is no evidence for differences among the genetic lineages concerning breeding system – all taxa appear to be outcrossing, assessed both via pollen/ovule ratios (Cruden, 1977; further details in Table S2 available as Supplementary online material) and genetic diversity (AWD, Table 1) –, pollination biology, flowering time or habitat requirements (Stuessy, 1972). Hence, their strong geographic structure likely is a remnant of geographic isolation (i.e., vicariance, as also suggested by the negative relationships of genetic and geographic distances) imposed on this xerophytic species during cooler and wetter periods in the Pleistocene. Such periods are known to have occurred during the last glacial maximum (between 20,000 and 14,000 years BP) in the Sonoran and Chihuahuan deserts (Metcalfe et al., 2000), in central Texas (Musgrove et al., 2001), and, although less pronounced, in the Tamaulipan Plains (Morafka, 1989; Morafka et al., 1992). They have strongly shaped the phylogeographic histories of both desert animals (e.g., Riddle and Hafner, 2006; Castoe et al., 2007) and desert plants (e.g., Nason et al., 2002; Fehlberg and Ranker, 2009; Garrick et al., 2009). Climate modeling suggests that during glacial time, desert shrubs such as *Fouquieria splendens* (Fouquieriaceae), which commonly accompany *M. cinereum* today, have remained absent from areas around the Rio Grande valley due to their higher winter temperature requirements (Holmgren et al., 2007). Although there are no known *Melampodium* fossils, the modeling data suggest that the vegetation type in which *M. cinereum* is currently found was much reduced during cooler and wetter periods. Xerophytic vegetation was probably reduced to pockets of higher temperatures as have been inferred for the Sonoran Desert (Holmgren et al., 2007) or,

Table 4
Marginal likelihoods, their Monte Carlo error, and the test statistic $2 \times \ln BF$ for different demographic models (constant population size, exponential population growth, two-epoch model, Bayesian Skyline Plot [BSP]) without (H1–H4) or with polyploids constrained to be monophyletic (H5–H8; see text for further details). The compared hypotheses (H and H^*) are arranged in rows and columns, respectively. $2 \times \ln BF_{H \text{ vs. } H^*} > 10$ is considered strong support for H, while $2 \times \ln BF_{H \text{ vs. } H^*} < -10$ is considered strong support for H^*.

	Marginal likelihood ± Monte Carlo error	$2 \times \ln BF$							
		H1	H2	H3	H4	H5	H6	H7	H8
H1: constant	−4946.513 ± 0.107		0.082	7.896	13.458	234.976	236.730	240.602	245.962
H2: exponential growth	−4946.554 ± 0.124	−0.082		7.814	13.376	234.894	236.648	240.520	245.880
H3: two–epochs	−4950.461 ± 0.121	−7.896	−7.814		5.562	227.080	228.834	232.706	238.066
H4: BSP	−4953.242 ± 0.116	−13.458	−13.376	−5.562		221.518	223.272	227.144	232.504
H5: constant + polyploids	−5064.001 ± 0.110	−234.976	−234.894	−227.080	−221.518		1.754	5.626	10.986
H6: exponential growth + polyploids	−5064.878 ± 0.114	−236.730	−236.648	−228.834	−223.272	−1.754		3.872	9.232
H7: two–epochs + polyploids	−5066.814 ± 0.115	−240.602	−240.520	−232.706	−227.144	−5.626	−3.872		5.360
H8: BSP + polyploids	−5069.494 ± 0.119	−245.962	−245.880	−238.066	−232.504	−10.986	−9.232	−5.360	

alternatively, might have persisted in mixtures with dry woodlands unusual today, but suggested for the lowest parts of the Chihuahuan Desert (van Devender, 1990). After the last glacial maximum, the whole region experienced progressive warming and drying, which started earlier in the Sonoran than in the Chihuahuan Desert (van Devender, 1990). This aridification, which might have happened gradually or in a stepwise manner and is possibly still ongoing (Holmgren et al., 2007), continued through the Holocene until the current semiarid climate had been established (Toomey et al., 1993; Bousman, 1998; Musgrove et al., 2001). The hypothesis of post-glacial colonization of newly formed xeric habitats from putatively small and isolated refugia established during cooler and wetter periods, as shown for Sonoran plant species (Nason et al., 2002; Fehlberg and Ranker, 2009; Garrick et al., 2009), is also supported by the inferred increase of effective population size around 0.015 Mya (Bayesian skyline plot, Fig. 6). Although this estimate as well as the one obtained from the mismatch distribution of 0.024 Mya likely are overestimates – because of the use of a presumably too slow substitution rate and the likely underestimation of recent substitution rates due to the time dependency of molecular rate estimates (Ho et al., 2005, 2007) – they are remarkably close to the onset of aridification suggested by paleoclimatic evidence (0.012–0.005 Mya; Holmgren et al., 2007).

Remarkably, the pattern of geographically distinct genetic lineages seen in the AFLP data (Figs. 2–4) is not reflected at all by the plastid data (Fig. 5), which instead show no significant variation among groups identified in the nuclear data (AMOVA; Table 2) and are highly diverse and partly strongly divergent within populations (Fig. 5). This results in a much higher within population variation (37%, Table 2) than in other species of southern North American xeric habitats (c. 9–28%: Fehlberg and Ranker, 2009; Garrick et al., 2009; Sosa et al., 2009). A lack of geographic structure and a high intrapopulational haplotype diversity would agree with long-term persistence of large populations, a scenario in line with the best supported demographic model of constant population size (Table 4), but contradicting the evidence from the AFLP data. If considering that the fast-evolving AFLP data likely trace more recent, (Late) Quaternary, events (Kropf et al., 2009), where commonly used plant DNA sequence markers provide insufficient or no resolution (Bussell et al., 2005; Meudt and Clarke, 2007), the observed patterns may reflect the signatures of populational processes at different time scales. This would imply that the observed intrapopulational haplotype diversity and heterogeneity are the result of lineage sorting during more recent periods of population separation, a hypothesis supported by the interior position of haplotypes in some of the variable populations (e.g., pops. 1 and 3, Fig. 5). A not mutually exclusive alternative is that, due to the lack of any major geographic barriers in the distribution area of *M. cinereum*, some gene flow between populations did occur, especially during warmer and drier periods (Allen and Anderson, 2000). In *M. cinereum*, gene flow via seeds might be enhanced by fruit morphology, as the fruits, which are derived exclusively from the ray florets, are enwrapped in hardened and hooked involucral bracts, suggesting that the diaspores might be dispersed epizoochorously. Extensive gene flow via seeds would also explain the weak signal in the plastid data for population size changes, resulting in a model of constant population size having the highest marginal likelihood, although more complex models allowing a recent increase in population size (exponential growth and a two-epoch model) cannot be rejected (Table 4). Whereas in plastid data a signal of recent or historical gene flow among populations is retained, AFLPs, which are homogenized more rapidly (due to repeated backcrossing of hybrids between resident and immigrant genotypes with the resident ones, Zhou et al., 2005), will reflect isolation in different refugia during the cooler and wetter phase of the last glacial maximum (Holmgren et al., 2007).

Some of the haplotypes (shown in Fig. 5) are shared with the closely related *M. leucanthum*, whose distribution range abuts that of *M. cinereum* in the Chihuahuan Desert. Neither morphological (Stuessy, 1971b, 1972) nor genetic data (Rebernig et al., unpublished data) provide any evidence for recent or ongoing hybridisation between these two species. Therefore, the haplotype sharing likely is due to ancient hybridisation and chloroplast capture, a common phenomenon in plants (Soltis et al., 1991, 1996; Okuyama et al., 2005). Removal of these haplotypes does not, however, change the overall pattern of high intrapopulational diversity and only weak geographic structure (data not shown).

Tetraploids are the sole cytotype in a compact area at the north-eastern edge of the distribution of *M. cinereum* (Fig. 1). Plastid data provide clear evidence that these polyploids originated recurrently (single origins are unambiguously rejected by Bayes factors; Table 4). A recurrent origin, most likely via unreduced gametes (Ramsey and Schemske, 1998, 2002; Leitch and Leitch, 2008), is also supported by the observation of occasional tetraploids throughout other parts of the species' range as well as the occasional occurrence of plants of higher ploidy level within lower-ploid populations (Stuessy et al., 2004; Obermayer et al., unpublished data). Although it cannot be entirely excluded, the alternative hypothesis of a single origin and subsequent inter-cytotype gene flow is less likely due to the lack of triploid hybrids between the two cytotypes (Stuessy et al., 2004; Obermayer and Weiss-Schneeweiss, unpublished data). Given the high intrapopulational haplotype diversity (Fig. 5), the origin of the tetraploids still could have taken place in a restricted area, as is also supported by the assignment tests of AFLP data, which identify a few diploid populations in the northern part of the distribution as the most likely source.

Despite its multiple origins, tetraploid *M. cinereum* var. *cinereum* is genetically cohesive (Figs. 2 and 3, S2) and occupies a compact distribution range to the exclusion of diploids (Fig. 1). One possible cause for polyploid establishment is ecological niche shift, which usually occurs outside or at the edge of the diploid range (Fowler and Levin, 1984; Felber, 1991; Baack and Stanton, 2005) in agreement with the current distribution patterns (Fig. 1). This hypothesis finds, however, little support, because there are no differences between the two cytotypes of var. *cinereum* concerning pollination, flowering time or habitat requirements (Stuessy, 1972). Since the establishment of tetraploid var. *cinereum* within diploid populations without ecological or other differentiation is unlikely based on theoretical considerations (minority cytotype disadvantage: Levin, 1975; Husband, 2000), we suggest that polyploid establishment in *M. cinereum* has been facilitated by geographic isolation, possibly in a period with less suitable climate (see above). Geographic isolation may have rendered the tetraploid locally dominant, thus reversing the minority cytotype disadvantage (Keeler and Davis, 1999). Once pure tetraploid populations are established, sharp boundaries between diploid and tetraploid populations may be maintained even on a local scale by reduced fitness of the offspring from inter-cytotype crosses (triploid block: Ramsey and Schemske, 1998; Hardy et al., 2001). Evidently, further studies are necessary to determine the actual dynamics at the contact zone between diploid and tetraploid *M. cinereum* var. *cinereum*.

Acknowledgments

The authors thank Cordula Blöch, Michael H.J. Barfuss, and Michael Lenko (University of Vienna, Austria), Monique Reed and Hugh Wilson (Texas A&M University, USA), and Donovan Bailey and Patrick Alexander (New Mexico State University, USA) for help with material collection. We thank Gudrun Kohl (University of Vienna, Austria) for technical assistance. We thank two anonymous reviewers for their comments, which greatly improved the paper. The study was financially supported by Austrian Science Fund (FWF) Grant No. P18201-B03 (to T.F.S.) and a Hertha-Firnberg postdoctoral fellowship T-218 (to H.W.S.).

Appendix A. Supplementary data

Supplementary data associated with this article can be found, in the online version, at doi:10.1016/j.ympev.2009.10.010.

References

Abbott, R.J., Brochmann, C., 2003. History and evolution of the arctic flora: in the footsteps of Eric Hultén. Mol. Ecol. 12, 299–313.
Allen, B.D., Anderson, R.Y., 2000. A continuous, high-resolution record of late Pleistocene climate variability from the Estancia basin, New Mexico. Geol. Soc. Am. Bull. 112, 1444–1458.
Baack, E.J., 2005. To succeed globally, disperse locally: a stochastic spatial model for tetraploid establishment. Heredity 94, 538–546.
Baack, E.J., Stanton, M.L., 2005. Ecological factors influencing tetraploid speciation in snow buttercups (*Ranunculus adoneus*): niche determination and tetraploid establishment. Evolution 59, 1936–1944.
Beheregaray, L.B., 2008. Twenty years of phylogeography: the state of the field and the challenges for the Southern Hemisphere. Mol. Ecol. 17, 3754–3774.
Bharathan, G., Lambert, G., Galbraith, D.W., 1994. Nuclear DNA content of monocotyledons and related taxa. Am. J. Bot. 81, 381–386.
Blöch, C., Weiss-Schneeweiss, H., Schneeweiss, G.M., Barfuss, M.H.J., Rebernig, C.A., Villaseñor, J.L., Stuessy, T.F., 2009. Molecular phylogenetic analyses of nuclear and plastid DNA sequences support dysploid and polyploid chromosome number changes and reticulate evolution in the diversification of *Melampodium* (Millerieae, Asteraceae). Mol. Phylogen. Evol. 53, 220–233.
Bohonak, A.J., van der Linde, K., 2004. RMA: Software for reduced major axis regression, Java version. Website: http://www.kimvdlinde.com/professional/rma.html.
Bonin, A., Bellemain, E., Eidesen, P.B., Pompanon, F., Brochmann, C., Taberlet, P., 2004. How to track and assess genotyping errors in population genetics studies. Mol. Ecol. 13, 3261–3273.
Bousman, B.C., 1998. Paleoenvironmental change in central Texas: the palynological evidence. Plains Anthropol. 43, 201–219.
Brunsfeld, S.J., Sullivan, J., Soltis, D.E., Soltis, P.S., 2001. Comparative phylogeography of northwestern North America: a synthesis. In: Silverton, J., Antonovics, J. (Eds.), Integrating Ecology and Evolution in a Spatial Context. Blackwell Science, Oxford, pp. 319–339.
Bussell, J.D., Waycott, M., Chappill, J.A., 2005. Arbitrarily amplified DNA markers as characters for phylogenetic inference. Persp. Plant Ecol. Evol. Syst. 7, 3–26.
Castoe, T.A., Spencer, C.L., Parkinson, C.L., 2007. Phylogeographic structure and historical demography of the western diamondback rattlesnake (*Crotalus atrox*): a perspective on North American desert biogeography. Mol. Phylogen. Evol. 42, 193–212.
Clark-Tapia, R., Molina-Freaner, F., 2003. The genetic structure of a columnar cactus with a disjunct distribution: *Stenocereus gummosus* in the Sonoran desert. Heredity 90, 443–450.
Clement, M., Posada, D., Crandall, K.A., 2000. TCS: a computer program to estimate gene genealogies. Mol. Ecol. 9, 1657–1660.
Corander, J., Marttinen, P., 2006. Bayesian identification of admixture events using multilocus molecular markers. Mol. Ecol. 15, 2833–2843.
Corander, J., Marttinen, P., Mäntyniemi, S., 2006. A Bayesian method for identification of stock mixtures from molecular marker data. Fishery Bull. 104, 550–558.
Cruden, R.W., 1977. Pollen-ovule ratios: a conservative indicator of breeding systems in flowering plants. Evolution 31, 32–46.
Dixon, C.J., 2006. A means of estimating the completeness of haplotype sampling using the Stirling probability distribution. Mol. Ecol. Notes 6, 650–652.
Dixon, C.J., Schönswetter, P., Schneeweiss, G.M., 2008. Morphological and geographical evidence are misleading with respect to the phylogenetic position and origin of the narrow endemic polyploid *Androsace cantabrica* (Primulaceae). Syst. Bot. 33, 384–389.
Dobeš, C.H., Mitchell-Olds, T., Koch, M.A., 2004. Extensive chloroplast haplotype variation indicates Pleistocene hybridization and radiation of North American *Arabis drummondii*, *A. xdivaricarpa* and *A. holboellii* (Brassicaceae).. Mol. Ecol. 13, 349–370.
Drummond, A.J., Ho, S.Y.W., Phillips, M.J., Rambaut, A., 2006. Relaxed phylogenetics and dating with confidence. PLoS Biol. 4 (5), e88. doi:10.1371/journal.pbio.0040088.
Drummond, A.J., Rambaut, A., 2007. BEAST: Bayesian evolutionary analysis by sampling trees. BMC Evol. Biol. 7, 214. doi:10.1186/1471-2148-7-214.
Drummond, A.J., Rambaut, A., Shapiro, B., Pybus, O.G., 2005. Bayesian coalescent inference of past dynamics from molecular sequences. Mol. Biol. Evol. 22, 1185–1192.
Duchesne, P., Bernatchez, L., 2002. AFLPOP: a computer program for simulated and real population allocation, based on AFLP data. Mol. Ecol. Notes 2, 380–383.
Ehrich, D., 2006. AFLPdat: a collection of R functions for convenient handling of AFLP data. Mol. Ecol. Notes 6, 603–604.
Ersts, P.J., 2009. Geographic Distance Matrix Generator (version 1.2.3). American Museum of Natural History, Center for Biodiversity and Conservation. Available from http://biodiversityinformatics.amnh.org/open_source/gdmg.
Excoffier, L., 2004. Patterns of DNA sequence diversity and genetic structure after a range expansion: lessons from the infinite-island model. Mol. Ecol. 13, 853–864.
Excoffier, L., Laval, L.G., Schneider, S., 2005. Arlequin (version 3.0): an integrated software package for population genetics data analysis. Evol. Bioinform. Online 1, 47–50.
Fehlberg, S.D., Ranker, T.A., 2009. Evolutionary history and phylogeography of *Encelia farinosa* (Asteraceae) from the Sonoran, Mojave, and Peninsular Deserts. Mol. Phylogen. Evol. 50, 326–335.
Felber, F., 1991. Establishment of a tetraploid cytotype in a diploid population: effect of relative fitness of the cytotypes. J. Evol. Biol. 4, 195–207.
Fowler, N.L., Levin, D.A., 1984. Ecological constraints on the establishment of a novel polyploid in competition with its diploid progenitor. Am. Nat. 124, 703–711.
Fu, X.Y., 1997. Statistical tests of neutrality of mutations against population growth, hitchhiking and background selection. Genetics 147, 915–925.
Garrick, R.C., Nason, J.D., Meadows, C.A., Dyer, R.J., 2009. Not just vicariance: phylogeography of a Sonoran Desert euphorb indicates a major role of range expansion along the Baja peninsula. Mol. Ecol. 18, 1916–1931.
Greilhuber, J., Obermayer, R., 1997. Genome size and maturity group in *Glycine max* (soybean). Heredity 78, 547–551.
Guo, Y.P., Saukel, J., Ehrendorfer, F., 2008. AFLP tree versus scatterplots: evolution and phylogeography of the polyploid complex *Achillea millefolium* agg. (Asteraceae). Taxon 57, 153–169.
Hall, T.A., 1999. BioEdit: a user-friendly biological sequence alignment editor and analysis program for Windows 95/98/NT. Nucl. Acids Symp. Ser. 41, 95–98.
Hardy, O.J., de Loose, M., Vekemans, X., Meerts, P., 2001. Allozyme segregation and inter-cytotype reproductive barriers in the polyploid complex *Centaurea jacea*. Heredity 87, 136–145.
Hewitt, G.M., 2001. Speciation, hybrid zones and phylogeography–or seeing genes in space and time. Mol. Ecol. 10, 537–549.
Hewitt, G.M., 2004. Genetic consequences of climatic oscillations in the Quaternary. Phil. Trans. R. Soc. Lond. B 359, 183–195.
Ho, S.Y.W., Phillips, M.J., Cooper, A., Drummond, A.J., 2005. Time dependency of molecular rate estimates and systematic overestimation of recent divergence times. Mol. Biol. Evol. 22, 1561–1568.
Ho, S.Y.W., Shapiro, B., Phillips, M.J., Cooper, A., Drummond, A.J., 2007. Evidence for time dependency of molecular rate estimates. Syst. Biol. 56, 515–522.

Holmgren, C.A., Norris, J., Betancourt, J.L., 2007. Inference about winter temperature and summer rains from the late Quaternary record of C_4 perennial grasses and C_3 desert shrubs in the northern Chihuahuan Desert. J. Quatern. Sci. 22, 141–161.

Husband, B.C., 2000. Constraints on polyploid evolution: a test of the minority cytotype exclusion principle. Proc. R. Soc. Lond. B 267, 217–223.

Husband, B., 2004. Polyploidy and plant adaptation: a framework for future research. In: Cronk, Q.C.B., Whitton, J., Ree, R.H., Taylor, I.E.P. (Eds.), Plant Adaptation: Molecular Genetics and Ecology. NRC Research Press, Ottawa, pp. 119–126.

Husband, B.C., Schemske, D.W., 2000. Ecological mechanisms of reproductive isolation and coexistence of diploid and tetraploid *Chamerion angustifolium*. J. Ecol. 88, 689–701.

Huson, D.H., Bryant, D., 2006. Application of phylogenetic networks in evolutionary studies. Mol. Biol. Evol. 23, 254–267.

Ingvarsson, P.K., Ribstein, S., Taylor, D.R., 2003. Molecular evolution of insertions and deletions in the chloroplast genome of *Silene*. Mol. Biol. Evol. 20, 1737–1740.

Jackson, R.C., Hauber, D.P., 1982. Autotriploid and autotetraploid cytogenetic analyses: correction coefficients for proposed binomial models. Am. J. Bot. 69, 644–646.

Jakobsson, M., Rosenberg, N.A., 2007. *CLUMPP*: a cluster matching and permutation program for dealing with label switching and multimodality in analysis of population structure. Bioinformatics 23, 1801–1806.

Kass, R.E., Raftery, A.E., 1995. Bayes factors. J. Am. Stat. Ass. 90, 773–795.

Keeler, K.H., Davis, G.A., 1999. Comparison of common cytotypes of *Andropogon gerardii* (Andropogoneae, Poaceae). Am. J. Bot. 86, 974–979.

Knowles, L.L., 2004. The burgeoning field of statistical phylogeography. J. Evol. Biol. 17, 1–10.

Knowles, L.L., Maddison, W.P., 2002. Statistical phylogeography. Mol. Ecol. 11, 2623–2635.

Kosman, E., 2003. Nei's gene diversity and the index of average differences are identical measures of diversity within populations. Plant Pathol. 52, 533–535.

Kropf, M., Comes, H.P., Kadereit, J.W., 2009. An AFLP clock for the absolute dating of shallow-time evolutionary history based on the intraspecific divergence of southwestern European alpine plant species. Mol. Ecol. 18, 697–708.

Leitch, A.R., Leitch, I.J., 2008. Genome plasticity and diversity of polyploid plants. Science 320, 481–483.

Leitch, I.J., Bennett, M.D., 1997. Polyploidy in angiosperms. Trends Plant Sci. 2, 470–476.

Leitch, I.J., Bennett, M.D., 2004. Genome downsizing in polyploid plants. Biol. J. Linn. Soc. 82, 651–663.

Levin, D.A., 1975. Minority cytotype exclusion in local plant populations. Taxon 24, 35–43.

Levin, D.A., 1983. Polyploidy and novelty in flowering plants. Am. Nat. 122, 1–25.

Levin, D.A., 2002. The Role of Chromosomal Change in Plant Evolution. Oxford University Press, New York, New York.

Löhne, C., Borsch, T., 2005. Molecular evolution and phylogenetic utility of the *pet*D group II intron: a case study in basal angiosperms. Mol. Biol. Evol. 22, 317–332.

Manni, F., Guérard, E., Heyer, E., 2004. Geographic patterns of (genetic, morphologic, linguistic) variation: how barriers can be detected by using Monmonier's algorithm. Hum. Biol. 76, 173–190.

McClaran, M.P., van Devender, T.R., 1995. The Desert Grassland. University of Arizona Press, Tucson, Arizona.

Metcalfe, S.E., O'Hara, S.L., Caballero, M., Davies, S.J., 2000. Records of late Pleistocene-Holocene climatic change in Mexico–a review. Quartern. Sci. Rev. 19, 699–721.

Meudt, H.M., Clarke, A.C., 2007. Almost forgotten or latest practice? AFLP applications, analyses and advances. Trends Plant Sci. 12, 106–117.

Meyers, L.A., Levin, D.A., 2006. On the abundance of polyploidy in flowering plants. Evolution 60, 1198–1206.

Minin, V.N., Bloomquist, E.W., Suchard, M.A., 2008. Smooth skyride through a rough skyline: Bayesian coalescent-based inference of population dynamics. Mol. Biol. Evol. 25, 1459–1471.

Morafka, D.J., 1989. An interdisciplinary definition of North America's Chihuahuan desert: is it desirable and obtainable? In: Kent, R.B., Harnapp, V.R. (Eds.), Yearbook. Conference of Latin Americanist Geographers. Louisiana State University, Baton Rouge, Louisiana, pp. 23–34.

Morafka, D.J., Adest, G.A., Reyes, L.M., 1992. Differentiation of North American deserts: a phylogenetic evaluation of a vicariance model. In: Darwin, S.P., Welden, A.L. (Eds.), Biogeography of Mesoamerica. Tulane Studies in Zoology and Botany Special Publication, New Orleans, Louisiana, pp. 195–226.

Musgrove, M., Banner, J.L., Mack, L.E., Combs, D.M., James, E.W., Cheng, H., Edwards, R.L., 2001. Geochronology of late Pleistocene to Holocene speleothems from central Texas: implications for regional paleoclimate. Geol. Soc. Am. Bull. 113, 1532–1543.

Nason, J.D., Hamrick, J.L., Fleming, T.H., 2002. Historical vicariance and postglacial colonization effects on the evolution of genetic structure in *Lophocereus*, a Sonoran desert columnar cactus. Evolution 56, 2214–2226.

Nei, M., Li, W.H., 1979. Mathematical model for studying genetic variation in terms of restriction endonucleases. Proc. Natl. Acad. Sci. USA 76, 5269–5273.

Okuyama, Y., Fujii, N., Wakabayashi, M., Kawakita, A., Ito, M., Watanabe, M., Murakami, N., Kato, M., 2005. Nonuniform concerted evolution and chloroplast capture: heterogeneity of observed introgression patterns in three molecular data partition phylogenies of Asian *Mitella* (Saxifragaceae). Mol. Biol. Evol. 22, 285–296.

Olson, D.M., Dinerstein, E., Wikramanayake, E.D., Burgess, N.D., Powell, G.V.N., Underwood, E.C., D'Amico, J.A., Itoua, I., Strand, H.E., Morrison, J.C., Loucks, C.J., Allnutt, T.F., Ricketts, T.H., Kura, Y., Lamoreux, J.F., Wettengel, W.W., Hedao, P., Kassem, K.R., 2001. Terrestrial ecoregions of the world: a new map of life on Earth. Bioscience 51, 933–938.

Otto, S.P., Whitton, J., 2000. Polyploidy incidence and evolution. Annu. Rev. Genet. 34, 401–437.

Pook, C.E., Wüster, W., Thorpe, R.S., 2000. Historical biogeography of the western rattlesnake (Serpentes: Viviperidae: *Crotalus viridis*), inferred from mitochondrial DNA sequence information. Mol. Phylogen. Evol. 15, 269–282.

Posada, D., Crandall, K.A., 1998. Modeltest: testing the model of DNA substitution. Bioinformatics 14, 817–818.

Pritchard, J.K., Stephens, M., Donnelly, P.J., 2000. Inference of population structure using multilocus genotype data. Genetics 155, 945–959.

Ramsey, J., Robertson, A., Husband, B., 2008. Rapid adaptive divergence in New World *Achillea*, an autopolyploid complex of ecological races. Evolution 62, 639–653.

Ramsey, J., Schemske, D.W., 1998. Pathways, mechanisms, and rates of polyploid formation in flowering plants. Annu. Rev. Ecol. Syst. 29, 467–501.

Ramsey, J., Schemske, D.W., 2002. Neopolyploidy in flowering plants. Annu. Rev. Ecol. Syst. 33, 589–639.

Redelings, B.D., Suchard, M.A., 2005. Joint Bayesian estimation of alignment and phylogeny. Syst. Biol. 54, 401–418.

Riddle, B.R., Hafner, D.J., 2006. A step-wise approach to integrating phylogeographic and phylogenetic bigeographic perspectives on the history of a core North American warm desert biota. J. Arid Environ. 66, 435–461.

Rogers, A.R., Harpending, H., 1992. Population growth makes waves in the distribution of pairwise genetic differences. Mol. Biol. Evol. 9, 552–569.

Rosenberg, N.A., Pritchard, J.K., Weber, J.L., Cann, H.M., Kidd, K.K., Zhivotovsky, L.A., Feldman, M.W., 2002. The genetic structure of human populations. Science 298, 2381–2385.

Sang, T., Crawford, D.J., Stuessy, T.F., 1997. Chloroplast DNA phylogeny, reticulate evolution and biogeography of *Paeonia* (Paeoniaceae). Am. J. Bot. 84, 1120–1136.

Schlüter, P.M., Harris, S.A., 2006. Analysis of multilocus fingerprint data sets containing missing data. Mol. Ecol. Notes 6, 569–572.

Schneider, S., Excoffier, L., 1999. Estimating of past demographic parameters from the distribution of pairwise differences when the mutation rates vary among sites: application to human mitochondrial DNA. Genetics 152, 1079–1089.

Schönswetter, P., Stehlik, I., Holderegger, R., Tribsch, A., 2005. Molecular evidence for glacial refugia of mountain plants in the European Alps. Mol. Ecol. 14, 3547–3555.

Shaw, J., Lickey, E.B., Schilling, E.E., Small, R.L., 2007. Comparison of whole chloroplast genome sequences to choose noncoding regions for phylogenetic studies in angiosperms: the tortoise and the hare III. Am. J. Bot. 94, 275–288.

Smith, C.I., Pellmyr, O., Althoff, D.M., Balcázar-Lara, M., Leebens-Mack, J., Segraves, K.A., 2008. Pattern and timing of diversification in *Yucca* (Agavaceae): specialized pollination does not escalate rates of diversification. Proc. Roy. Soc. London B 275, 249–258.

Soltis, D.E., Albert, V.A., Leebens-Mack, J., Bell, C.D., Paterson, A.H., Zheng, C., Sankoff, D., dePamphilis, C.W., Wall, P.K., Soltis, P.S., 2009. Polyploidy and angiosperm diversification. Am. J. Bot. 96, 336–348.

Soltis, D.E., Johnson, L.A., Looney, C., 1996. Discordance between ITS and chloroplast topologies in the *Boykinia* group (Saxifragaceae). Syst. Bot. 21, 169–176.

Soltis, D.E., Mayer, M.S., Soltis, P.S., Edgerton, M., 1991. Chloroplast DNA variation in *Tellima grandiflora* (Saxifragaceae). Am. J. Bot. 78, 1379–1390.

Soltis, D.E., Morris, A.B., McLachlan, J.S., Manos, P.S., Soltis, P.S., 2006. Comparative phylogeography of unglaciated eastern North America. Mol. Ecol. 15, 4261–4293.

Sosa, V., Ruiz-Sanchez, E., Rodriguez-Gomez, F.C., 2009. Hidden phylogeographic complexity in the Sierra Madre Oriental: the case of the Mexican tulip poppy *Hunnemannia fumariifolia* (Papaveraceae). J. Biogeogr. 36, 18–27.

Stuessy, T.F., 1971a. Systematic relationships in the white-rayed species of *Melampodium* (Compositae). Brittonia 23, 177–190.

Stuessy, T.F., 1971b. Chromosome numbers and phylogeny in *Melampodium* (Compositae). Am. J. Bot. 58, 732–736.

Stuessy, T.F., 1972. Revision of the genus *Melampodium* (Compositae: Heliantheae). Rhodora 74, 1–70, 161–219.

Stuessy, T.F., Weiss-Schneeweiss, H., Keil, D.J., 2004. Diploid and polyploid cytotype distribution in *Melampodium cinereum* and *M. leucanthum* (Asteraceae, Heliantheae). Am. J. Bot. 91, 889–898.

Suchard, M.A., Weiss, R.E., Dorman, K.S., Sinsheimer, J.S., 2003. Inferring spatial phylogenetic variation along nucleotide sequences: a multiple change-point model. J. Am. Stat. Ass. 98, 427–437.

Suchard, M.A., Weiss, R.E., Sinsheimer, J.S., 2001. Bayesian selection of continuous-time Markov chain evolutionary models. Mol. Biol. Evol. 18, 1001–1013.

Suchard, M.A., Weiss, R.E., Sinsheimer, J.S., 2005. Models for estimating Bayes factors with applications to phylogeny and tests of monophyly. Biometrics 61, 665–673.

Suda, J., Krahulcová, A., Trávníček, P., Krahulec, F., 2006. Ploidy level versus DNA ploidy level: an appeal for consistent terminology. Taxon 55, 447–450.

Suda, J., Krahulcová, A., Trávníček, P., Rosenbaumová, R., Peckert, T., Krahulec, F., 2007. Genome size variation and species relationships in *Hieracium* subgen. *Pilosella* (Asteraceae) as inferred by flow cytometry. Ann. Bot. 100, 1323–1335.

Suda, J., Trávníček, P., 2006. Reliable DNA ploidy determination in dehydrated tissues of vascular plants by DAPI flow cytometry - new prospects for plant research. Cytometry A 69A, 273–280.

Tajima, F., 1996. The amount of DNA polymorphism maintained in a finite population when the neutral mutation rate varies among sites. Genetics 143, 1457–1465.

Tamura, K., Dudley, J., Nei, M., Kumar, S., 2007. MEGA4: molecular evolutionary genetics analysis (MEGA) software version 4.0. Mol. Biol. Evol. 24, 1596–1599.

Tate, J.A., Simpson, B.B., 2003. Paraphyly of *Tarasa* (Malvaceae) and diverse origins of the polyploid species. Syst. Bot. 28, 723–737.

Taulman, J.F., Robbins, L.W., 1996. Recent range expansion and distributional limits of the nine-banded armadillo (*Dasypus novemcinctus*) in the United States. J. Biogeogr. 23, 635–648.

Tel-Zur, N., Abbo, S., Myslabodski, D., Mizrahi, Y., 1999. Modified CTAB procedure for DNA isolation from epiphytic cacti of the genera *Hylocereus* and *Selenicereus* (Cactaceae). Plant Mol. Biol. Rep. 17, 249–254.

Toomey, R.S.I., Blum, M.D., Valastro, S., 1993. Late Quaternary climate and environments of the Edwards Plateau, Texas. Glob. Planet. Change 7, 299–320.

Van de Peer, Y., de Wachter, R., 1994. TREECON for Windows: a software package for the construction and drawing of evolutionary trees for the Microsoft Windows environment. Comp. Appl. Biosci. 10, 569–570.

Van Devender, T.R., 1990. Late Quaternary vegetation and climate of the Chihuahuan Desert, United States and Mexico. In: Betancourt, J.L., van Devender, T.R., Martin, P.S. (Eds.), Packrat Middens – The Last 40,000 Years of Biotic Change. University of Arizona Press, Tuscon, Arizona, pp. 104–133.

Vekemans, X., Beauwens, T., Lemaire, M., Roldan-Ruiz, I., 2002. Data from amplified fragment length polymorphism (AFLP) markers show indication of size homoplasy and a relationship between degree of homoplasy and fragment size. Mol. Ecol. 11, 139–151.

Waltari, E., Hijmans, R.J., Peterson, A.T., Nyári, Á.S., Perkins, S.L., Guralnick, R.P., 2007. Locating Pleistocene refugia: comparing phylogeographic and ecological niche model predictions. PLoS One 2 (7), e563. doi:10.1371/journal.pone.0000563.

Weiss-Schneeweiss, H., Schneeweiss, G.M., Stuessy, T.F., Mabuchi, T., Park, J.M., Jang, C.G., Sun, B.Y., 2007. Chromosomal stasis in diploids contrasts with genome restructuring in auto- and allopolyploid taxa of *Hepatica* (Ranunculaceae). New Phytol. 174, 669–682.

Weiss-Schneeweiss, H., Stuessy, T.F., Villaseñor, J.L., 2009. Chromosome number, karyotypes, and evolution in Melampodium (Asteraceae). Int. J. Plant Sci. 170, 1168–1182.

Wendel, J.F., 2000. Genome evolution in polyploids. Plant Mol. Biol. 42, 225–249.

Yamane, K., Yasui, Y., Ohnishi, O., 2003. Intraspecific cpDNA variations of diploid and tetraploid perennial buckwheat, *Fagopyrum cymosum* (Polygonaceae). Am. J. Bot. 90, 339–346.

Zhivotovsky, L.A., 1999. Estimating population structure in diploids with multilocus dominant DNA markers. Mol. Ecol. 8, 903–913.

Zhou, R., Shi, S., Wu, C.I., 2005. Molecular criteria for determining new hybrid species – an application to the *Sonneratia* hybrids. Mol. Phylogen. Evol. 35, 595–601.